

APPLICATION NOTE

Two-Photon Excited Fluorescence Microscopy

32

Technology and Applications Center
Newport Corporation

Introduction

Several laser-scanning microscopy techniques have been developed in the last twenty years based on non-linear optical phenomena.¹ This has led to a variety of powerful imaging tools, such as two-photon excited fluorescence microscopy (TPM),² second harmonic generation (SHG) microscopy,³ and coherent anti-Stokes Raman scattering (CARS) microscopy.⁴ The advantages these novel techniques present versus conventional microscopy methods have enabled great developments in biological imaging, especially in thick tissue and live animal studies.

The common denominator of these techniques, which can be grouped in the family of multiphoton microscopy (MPM), is the non-linear dependence of the signal with the intensity of the excitation light. Some of the consequences of this phenomenon are the localization of signal within a femtoliter volume, the reduction of photodamage in out-of-focus planes, and the ability to excite areas hundreds of microns deep within samples.

While microscopy by SHG and CARS has shown great potential in biological imaging because extrinsic fluorescent molecules are not required for signal generation, TPM thus far has seen wider use. The discovery of the Green Fluorescent Protein has further increased the imaging capabilities of TPM. By fusing auto-fluorescent proteins to proteins of interest, TPM can perform imaging of complex cellular processes down to the single molecule level.^{5,6}

Two-Photon Absorption

A molecule in a ground electronic state can be promoted to an excited vibronic state if it absorbs a photon with energy matching the energy gap between the two states. After relaxing to the lower vibrational state, the molecule will return to the ground electronic state emitting a lower energy photon than the one absorbed. This is the basis of one-photon excited fluorescence. The difference in frequency between the photon absorbed and the photon emitted is called the Stokes shift.

The same process can occur by quasi-simultaneous absorption of two lower energy photons via short-lived virtual states, if the energy sum of the two photons is enough to reach the first excited electronic state. In this case, the probability of absorption is proportional to the intensity squared of the excitation light.



Figure 1 – Picture of the setup for TPM.

Two-photon absorption is a rare event.⁷ In order to increase its probability, intense sources of light are required. It is not surprising then that the first experimental evidence of two-photon absorption occurred after the invention of lasers that provided sufficient photon densities in collimated beams.⁸

Although two-photon absorption can be induced by using CW lasers, pulsed lasers are preferable because they can achieve the same excitation efficiencies with much lower average powers due to high peak intensity. It can be shown that in order to induce the same fluorescence signal, the power of a CW laser has to be $(\tau_p f_p)^{-1/2}$ higher than the average power of a pulsed laser where τ_p and f_p are the pulse width and the repetition rate respectively. For example the fluorescence intensity emitted by a fluorophore through two-photon absorption will be about the same, whether a 10 W continuous-wave laser or a 30 mW from a typical commercial femtosecond pulsed laser is employed.⁹

Focusing is as important as the use of an intense source of light for inducing two-photon absorption. In order to increase the probability of having two photons simultaneously at the same place and hence increase the probability of absorption, high numerical aperture objectives are used to focus the laser beam to a diffraction limited spot. Since two-photon absorption is proportional to the intensity squared of the excitation light, fluorescence signal induced by two-photon absorption is greatly enhanced by focusing the laser beam.

Advantages of Two-Photon Microscopy

In the seminal paper by Webb and co-workers describing TPM¹⁰, a relationship between the probability of two-photon absorption by a single molecule and measurable experimental parameters was presented. The probability per pulse that a fluorophore will undergo excitation by two-photon absorption when it is illuminated by a train of pulses through a focusing lens is given by

$$n_a \propto \frac{\delta_2 P_{ave}^2}{\tau_p f_p^2} \left(\frac{NA^2}{2\hbar c \lambda} \right)^2 \quad (1)$$

where δ_2 is the two-photon cross-section of the fluorophore at wavelength λ , P_{ave} the laser beam average power, NA the numerical aperture of the focusing lens, \hbar is the reduced Plank constant, and c the speed of light. In a typical experiment, the laser average power and pulse width are set carefully in order to maximize signal generation. It is important to avoid saturation ($n_a \approx 1$), otherwise the image will lose the optical resolution defined by the numerical aperture of the focusing lens and the excitation wavelength.

The fluorescence signal produced in TPM is proportional to the probability of two-photon absorption. Since this event scales with the laser intensity squared, two-photon excited fluorescence can be spatially confined by focusing the excitation light.

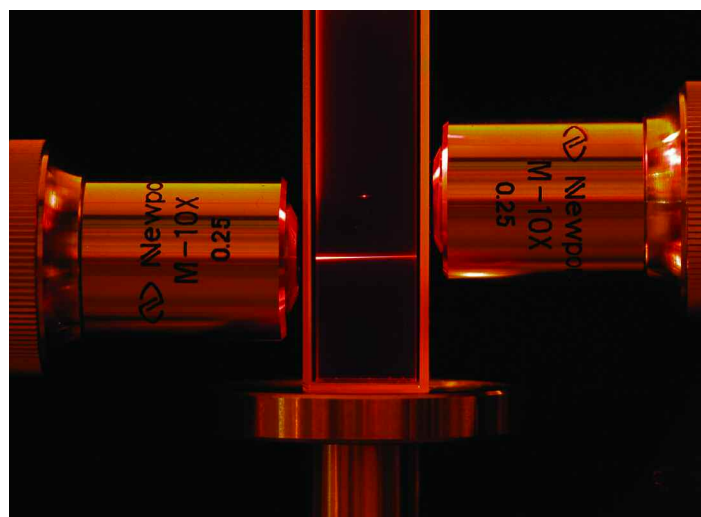
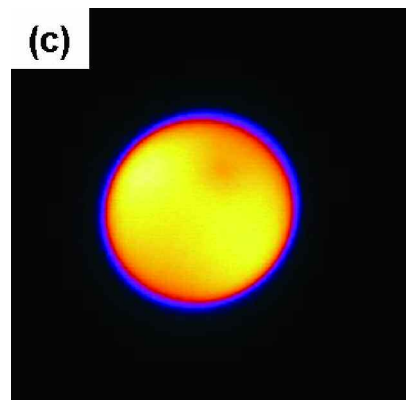
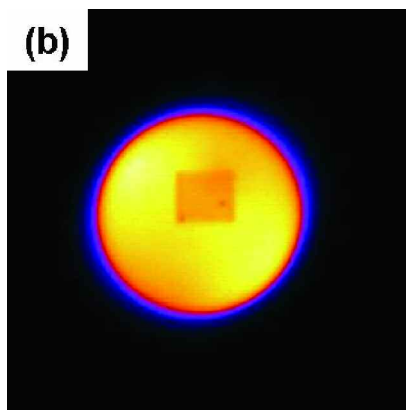
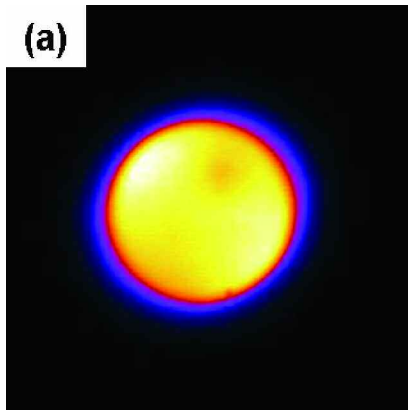


Figure 2 – An experiment demonstrating the difference between one- and two-photon induced fluorescence.

The integration of two-photon absorption probability over sections of the illuminating cone is largest at the focal plane and dies off rapidly in the regions in front and behind it. The confinement of excitation and thus signal production in a small volume within samples is certainly the key feature of TPM. It is demonstrated in Figure 2 by comparing the effect of one- and two-photon absorption on signal generation. The cuvette contains a solution of Rhodamine B in Methanol. The objective on the left is focusing 405 nm light from a CW diode laser while the objective on the right is focusing 800 nm light from a femtosecond pulsed laser. When the solution is excited by a one-photon process at 405 nm, fluorescence is generated everywhere along the optical axis. Upon two-photon absorption at 800 nm, fluorescence is observed exclusively at the focal point of the objective. By using high numerical aperture objectives, fluorescence induced by two-photon absorption can be confined to only a few hundred nanometers of path length, enabling high resolution imaging with low out-of-focus background.

Another advantage of TPM is the ability to image thick samples, even when they are highly heterogeneous. This is due to the use of longer wavelengths (near IR) relative to shorter ones (visible and UV) used in conventional one-photon fluorescence microscopy. Since light scattering is proportional to λ^{-4} , TPM photons can reach deeper into samples and not be lost. With appropriate objectives, TPM has been used to image biological events up to several hundred microns within dense tissues.¹¹ The high penetration depth of TPM is further enhanced because most biological samples present little linear absorption between 700 and 1000 nm.

During signal collection in fluorescence microscopy, filters are used to block the back-scattered excitation photons from reaching the detector. Since the Stokes shift is not large enough to separate emission from excitation in single-photon processes for most fluorophores, some fluorescence signal is lost through absorption by the filter. In TPM, emission and excitation wavelengths are well separated spectrally, thus enabling efficient signal collection.



When fluorophores are excited by either a one- or a two-photon absorption process, they may stop emitting fluorescent light if the intensity of the excitation light is too high or the exposure time is too long. This event, termed photobleaching, is caused by photon-induced chemical damage of the molecular structure of the fluorophore. It results in a decrease of signal in fluorescent microscopy. Although photobleaching can be minimized by changing the experimental conditions accordingly, signal degradation after imaging is always present to a certain extent. Since fluorescence induced by two-photon absorption is three-dimensionally confined, the effect of photobleaching in TPM is also spatially confined. This is an inherent advantage over confocal microscopy where the three-dimensionality of the signal is made possible by the presence of a pinhole in front of the detector, thereby rejecting photons generated outside the focal plane. In confocal microscopy, any part of the sample along the optical axis of the excitation light may sustain photobleaching due to linear absorption, while in TPM, photobleaching is confined to the focal plane only.

Figure 3 shows sections of a fluorescent polystyrene bead 20 micron in diameter recorded by TPM. Before imaging, the laser was scanned in a 6 by 6 micron area inside the bead using intentionally higher laser intensity than required for imaging, thus enhancing the effect of photobleaching. The three sections were then imaged three microns above, three microns below, and in the plane where photobleaching occurred. As expected, no effects of photobleaching are visible in Figures 3(a) and 3(c) while a dark square is present in Figure 3(b).

Besides photobleaching, the use of high laser intensities for imaging can cause other undesirable photodamage processes. Heat, ablation, and formation of singlet oxygen will all have irreversible effects on samples. By using near-IR photons and by constricting absorption to only the focal volume, TPM permits imaging of events in biological specimens without compromising their viability. In a recent study, TPM and linear confocal microscopy were used to image hamster embryos at several stages of their growth. Only by using TPM, were the embryos able to grow to become mature animals; the degree of photodamage caused by imaging with confocal microscopy was fatal.¹²

Figure 3 – Cross-section images in false colors of a fluorescent polystyrene beads 20 μm in diameter. Figure (a), (b), and (c) were recorded with the focal plane at three different depths within the bead, with a separation of 3 μm .

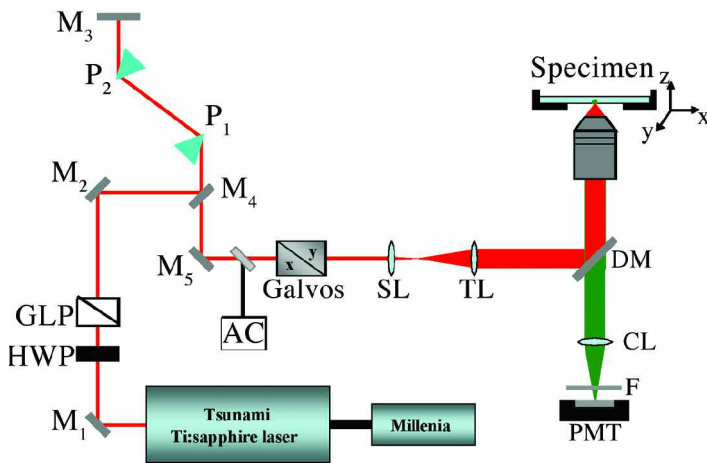


Figure 4 – Schematic of the experimental setup used in this application note. HWP, half-wave plate; GLP, Glan-laser polarizer; M, mirror; P, prism; AC, autocorrelator; SL, scanning lens; TL, tube lens; DM, dichroic mirror; CL, collection lens; F, filter; PMT, photomultiplier tube.

Experimental Setup

The results presented in this application note were collected using an experimental setup (Figure 1) based, in part, on a design described elsewhere.¹³ The schematic diagram of the setup is illustrated in Figure 4.

The source of light is a Ti:Sapphire oscillator (Tsunami; www.newport.com/tsunami) that is pumped by a solid-state green laser (Millennia®; www.newport.com/Millennia) to produce femtosecond pulses at a repetition rate of 80 MHz. The center wavelength of the emission light can be tuned between 700 and 1040 nm, and maximum output power is obtained at 800 nm.

A half-wave plate and a polarizer are positioned after the oscillator and are used to variably attenuate the laser output power to the desired input required by specific experiments. The laser beam is then steered into a prism compressor assembly that introduces enough dispersion compensation to ensure that the shortest pulses arrive at the sample. For more details on how to assemble and setup a variable power attenuator and a prism compressor, please see Application Notes 26 and 29 respectively (www.newport.com/appnotes)

A small portion of the laser beam is then directed to a beam diagnostic unit. In this setup, the laser pulse is characterized both in the time and frequency domain by employing the Newport PulseScout™ autocorrelator and spectrometer (www.newport.com/pulsecout).

A series of metallic mirrors route the laser beam to the scanning head. The scanning head includes two mirrors driven by galvanometers and two lenses. The set of galvo mirrors scan the laser beam in a raster fashion. The two lenses expand the beam diameter to maximize resolution, while their positioning reduces power losses at the back aperture of the objective while scanning.

After the scanning head, the laser enters an inverted microscope through a side port. A dichroic mirror, which is reflective for near-IR and transparent for visible radiation, deflects the laser beam into an infinity corrected objective that focuses the excitation light into the sample. The sample's position in the objective field of view is adjusted by the aid of a three axis computer-controlled stage.

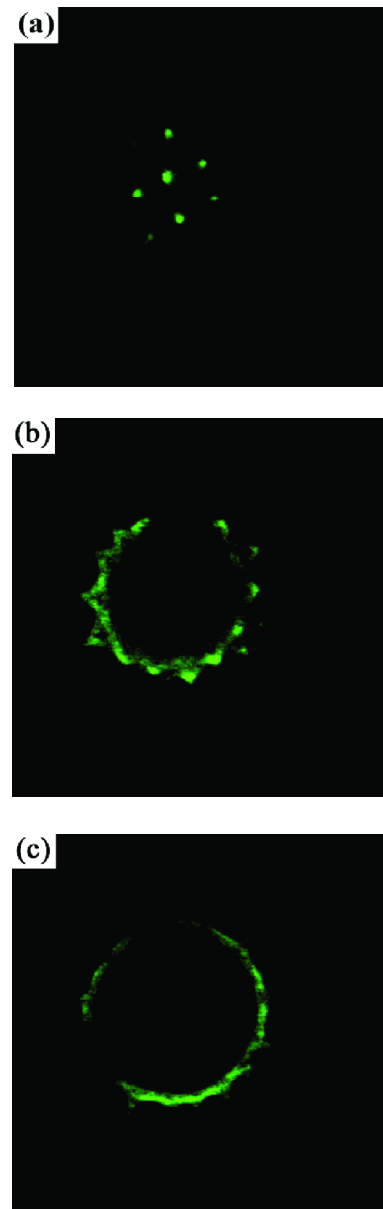


Figure 5 – Images of a pollen grain 30 μm in diameter recorded by TPM. The separation in depth between (a), (b), and (c) is 4 μm .

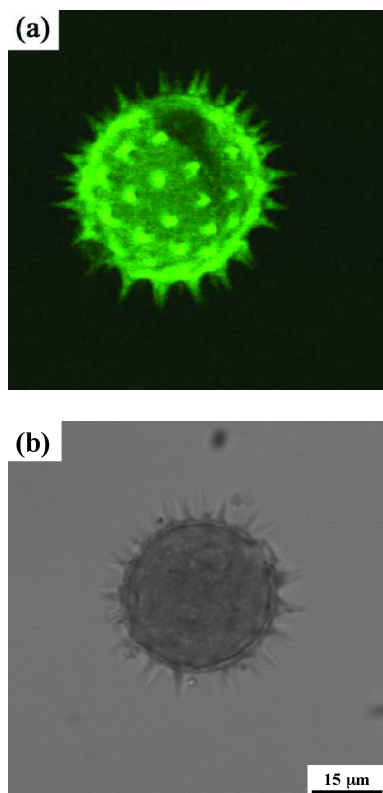


Figure 6 – TPM fluorescent (a) and wide-field microscopy (b) images of a pollen grain. Figure (a) was obtained by stacking together images of the pollen grain cross-section.

Fluorescence generated at the focal point is collected by the same objective used for excitation and passed through the dichroic mirror in a collimated fashion. A lens is then used to focus the emitted fluorescence onto the active area of a photomultiplier tube (PMT).

A computer workstation running MPscope software controls the scanning mirrors and collects the signal from the PMT.¹⁴ An image of the section of the specimen that is scanned is retrieved by synchronizing the position of the scanning mirrors at the moment photons are detected by the PMT. The scanning area is divided into a grid of pixels, each of which is assigned a color of the gray-scale palette relative to the signal intensity measured for that pixel. In this way, a crisp image of the sample can be generated. By repeating this process at different depths, a three-dimensional rendering of the sample can be obtained.

In order to demonstrate its sectioning capabilities, TPM was employed to image a pollen grain. This specimen is 30 μm in diameter and it is characterized by the presence of spikes on its surface. Figure 5 shows images of three sections of the pollen grain that were acquired by recording the autofluorescence at different depths using 800 nm excitation at 10 mW average power. Information on the specimen can be gained section by section without cross-talk among them. Furthermore, three-dimensional reconstruction of the sample can be performed in TPM by properly interpolating the recorded images. Figure 6(a) illustrates the result of this operation in the case of the pollen grain. For comparison, an image of the same specimen recorded in wide-field microscopy is shown in Figure 6(b)

Effect of excitation laser pulse width on TPM

The amount of signal collected in TPM can be augmented by increasing the average power of the excitation light source. Such a measure should be taken with care though, since it could induce two undesirable effects on imaging. One is the loss of optical resolution as a consequence of saturation. The other one is heating damage to the sample caused by linear absorption of near-IR photons. The second effect is of great concern for deep tissue imaging, or when studying living biological samples.

An inverse relationship exists between the probability of two-photon absorption and the pulse width (τ_p) of the laser (Eq. 1). Consequently, TPM signal can be heightened by increasing the peak power of the pulsed laser. This is accomplished by delivering the shortest pulses at the focal point of the imaging plane.

Ti:Sapphire oscillators used in TPM are capable of producing transform-limited femtosecond pulses. In this case, the time-bandwidth product is at its minimum and the frequencies within the spectrum of the pulse are temporally overlapping. Since most materials introduce positive dispersion in the visible and near-IR region of the spectrum, the transform-limited pulse of a Ti:Sapphire oscillator will be broadened in time when traveling through optical components. Called positive chirping, this phenomenon is characterized by the red frequencies of the pulse preceding the blue ones.

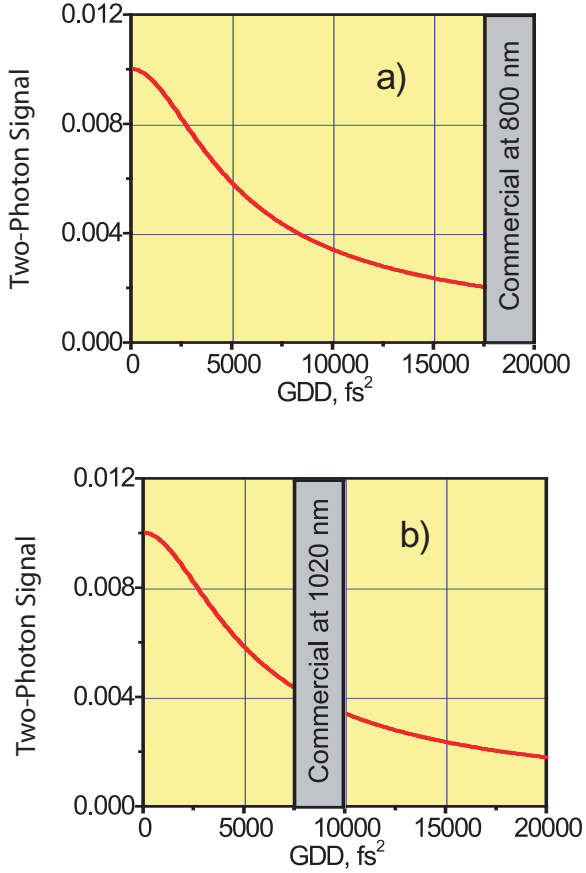


Figure 7 – Calculated two-photon excited fluorescence as function of group velocity dispersion at 800 nm (a) and 1020 nm (b). The signals are simulated with 100 fs input pulse

For a Gaussian transform-limited pulse, the amount of broadening the pulse will sustain when traveling through optical elements is given by

$$\tau_{out} = \tau_{in} \left[1 + 7.68 \left(\frac{D}{\tau_{in}^2} \right)^2 \right]^{\frac{1}{2}} \quad (2)$$

where τ_{in} and τ_{out} are the values of the pulse width before and after broadening and D is the group delay dispersion (GDD) of the system in units of femtosecond squared. The value of D in TPM systems can vary from 3,000 fs² to 40,000 fs². It depends on several factors, such as the objective employed to focus the excitation light, the operating wavelength, and the thickness and nature of the optical materials that the light goes through to reach the sample.

In order to ensure the shortest pulse at the sample, compensation of the positive dispersion has to be implemented in the setup for TPM. For systems where most of the dispersion is caused by the compound lens in the objective, a simple and compact, linear prism compressor is enough. In commercial systems where highly dispersive elements such as electro-optic or acousto-optic modulators are used, a compressor with much higher dispersion compensation range is required.^{15, 16}

By using equations (1) and (2), the dispersion effect that a specific amount of optical material has on the signal generated in TPM can be calculated. Two examples of these calculations are shown in Figure 7 where fluorescence signal induced by two-photon absorption is plotted as a function of GDD for 100 fs long pulses at two different excitation wavelengths.

The GDD of a typical basic system used for TPM is on the order of 5,000 fs², while for some commercial systems it can be as high as 40,000 fs². It is evident that at 800 nm, typical commercial systems require significantly higher average power to recover the signal lost to pulse broadening – with potential negative effects on cell viability when imaging live tissue in vivo or in vitro.

When considering pulses shorter than 30 fs at the sample, it's important to remember that they are accompanied by a large bandwidth. Most microscope objectives are not able to correct for the chromatic aberrations that occur when focusing such short pulses, resulting in poor optical resolution and decreased peak power at the focal point. Furthermore, when using sub-30 femtosecond pulses, the induced two-photon absorption process can become inefficient since absorption bands of fluorophores are smaller than the bandwidth of the excitation light.

The dispersion introduced by the basic microscope setup shown in Figure 1 was measured at 800 nm and found to be around 5,000 fs².

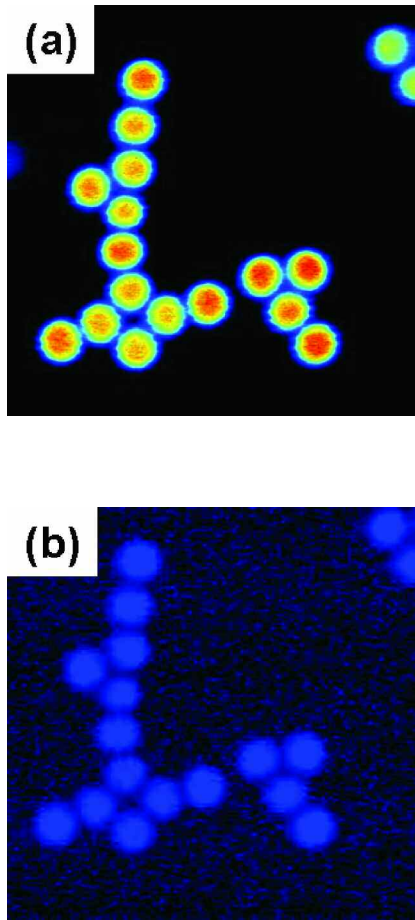


Figure 8 – False colored images of 2 μm diameter fluorescent polystyrene beads recorded by TPM at 800 nm. In Figure 8(a) the dispersion of the microscope set-up has been compensated using a prism compressor in order to deliver the shortest pulse at the sample. In Figure 8(b) the fluorescent signal of the same beads is greatly decreased by adding a large amount of dispersion. This time, the prism compressor cannot compensate such dispersion.

Figure 8 shows images of a sample consisting of fluorescent polystyrene beads. The two images were recorded with a 100x 1.3 numerical aperture objective using identical excitation conditions at 800 nm. In Figure 8(a), the prism compressor was adjusted to deliver the shortest pulses at the sample and hence produce the brightest image. The image in Figure 8(b) was acquired with a large block of glass corresponding to 20,000 fs^2 GDD inserted in the beam path before the microscope. This time, the amount of dispersion was too large to be compensated by the prism compressor used in the

TAC. With the same average power at the sample used for obtaining Figure 8(a), the decrease in signal in Figure 8(b) is evident. A full recovery of fluorescence was possible only by increasing the average power from 7 mW to 20 mW.

Recently Spectra-Physics introduced Mai Tai® DeepSee™ (www.newport.com/MaiTaiDeepSee), a compact, single-box femtosecond oscillator with integrated dispersion compensation. It is capable of compensating GDD up to 36,000 fs^2 – more than enough for maintaining short pulse width at the sample for most commercially available microscopes. The Mai Tai DeepSee is fully automated and optimizes images at different wavelength at the push of a button while maintaining the beam pointing into the microscope – the perfect light source for deep tissue and live cell multiphoton imaging.^{17, 18}

Conclusions

In this application note, we described several properties of TPM. We presented results that highlight the advantages of TPM over conventional microscopy techniques. We also provided data that allows users to decide whether compensating for dispersion is required or not in their imaging systems.

References

1. Zipfel W. R., Williams R. M., Webb W. W. *Nat. Biotech.* **21**, 1369 (2003)
2. So P. T. C., Dong C. Y., Masters B. R., Berland K. M. *Annu. Rev. Biomed. Eng.* **2**, 399 (2000)
3. Campagnola P. J., Clark H. A., Mohler W. A., Lewis W. A., Loew L. M. *J. Biomed. Opt.* **6**, 277 (2001)
4. Zumbusch A., Holtom G. R., Xie X. S. *Phys. Rev. Lett.* **82**, 4014 (1999)
5. Chalfie M., Tu Y., Euskirchen G., Ward W. W., Prasher D. C. *Science* **263**, 802 (1994)
6. D'appuzzo M., Mandolesi G., Reis G., Schuman E. M. *J. Neurophysiol.* **86**, 1037 (2001)
7. Denk S., Svoboda K. *Neuron* **18**, 351 (1997)
8. Kaiser W., Garret C. G. B. *Phys. Rev. Lett.* **7**, 229 (1961)
9. Diaspro A., Sheppard C. J. R. in *Confocal and Two-Photon Microscopy: Foundations, Applications, and Advances* (ed. Diaspro A.) 39 (Wiley-Liss, 2002)
10. Denk W., Strickler J. H., Webb W. W. *Science* **248**, 73 (1990)
11. Theer P., Hasan M. T., Denk W. *Opt. Lett.* **28**, 1022 (2003)
12. Squirrel J. M., Wokosin D. L., White J. G., Bavister B. D. *Nat. Biotechnol.* **17**, 763 (1999)
13. Tsai P. S., Nishimura N., Yoder E. J., Donlick E. M., White G. A., Kleinfeld D. in *In Vivo Optical Imaging of Brain Function* (ed. Frostig R. D.) 113, (CRC Press, 2002)
14. Nguyen Q.-T., Tsai P. S., Kleinfeld D. *J. Neurosci. Methods* **156**, 351 (2006)
15. Wollescensky R., Feurer T., Sauerbrey R., Simon U. *Appl. Phys. B* **67**, 87 (1998)
16. Squier J., Muller M. *Rev. Scient. Instr.* **72**, 2855 (2001)
17. David V., Krueger A., Feru P. *Laser Focus World* January 2007
18. David V., Feru P. *Biophotonics International* January 2007

Newport Corporation

Worldwide Headquarters

1791 Deere Avenue
Irvine, CA 92606

(In U.S.): 800-222-6440

Tel: 949-863-3144

Fax: 949-253-1680

Email: sales@newport.com



Newport

Experience | Solutions



Visit Newport Online at: www.newport.com

This Application Note has been prepared based on development activities and experiments conducted in Newport's Technology and Applications Center and the results associated therewith. Actual results may vary based on laboratory environment and setup conditions, the type and condition of actual components and instruments used and user skills.

Nothing contained in this Application Note shall constitute any representation or warranty by Newport, express or implied, regarding the information contained herein or the products or software described herein. Any and all representations, warranties and obligations of Newport with respect to its products and software shall be as set forth in Newport's terms and conditions of sale in effect at the time of sale or license of such products or software. Newport shall not be liable for any costs, damages and expenses whatsoever (including, without limitation, incidental, special and consequential damages) resulting from any use of or reliance on the information contained herein, whether based on warranty, contract, tort or any other legal theory, and whether or not Newport has been advised of the possibility of such damages.

Newport does not guarantee the availability of any products or software and reserves the right to discontinue or modify its products and software at any time. Users of the products or software described herein should refer to the User's Manual and other documentation accompanying such products or software at the time of sale or license for more detailed information regarding the handling, operation and use of such products or software, including but not limited to important safety precautions.

This Application Note shall not be copied, reproduced, distributed or published, in whole or in part, without the prior written consent of Newport Corporation.

Copyright ©2007 Newport Corporation. All Rights Reserved.



ISO 9001
FM 27207

Newport Corporation, Irvine, California, has been certified compliant with ISO 9001 by the British Standards Institution.

MM#00000092
DS-04071